atmosphere

MDPI

Article

Possible Identification of Precursor ELF Signals on Recent EQs That Occurred Close to the Recording Station

Ioannis Contopoulos [1,*], Janusz Mlynarczyk [2], Jerzy Kubisz [3] and Vasilis Tritakis [1,4,*]

[1] Research Center for Astronomy and Applied Mathematics, Academy of Athens, 15126 Athens, Greece
[2] Institute of Electronics, AGH University of Krakow, 30-059 Krakow, Poland; januszm@agh.edu.pl
[3] Astronomical Observatory, Jagiellonian University, 30-244 Krakow, Poland; kubisz@oa.uj.edu.pl
[4] Mariolopoulos-Kanaginis Foundation for Environmental Science, 10675 Athens, Greece
* Correspondence: icontop@academyofathens.gr (I.C.); vtritakis@academyofathens.gr (V.T.)

Abstract: The **Lithospheric–Atmospheric–Ionospheric Coupling (LAIC) mechanism** stands as the leading model for the prediction of seismic activities. It consists of a cascade of physical processes that are initiated days before a major earthquake. The onset is marked by the discharge of ionized gases, such as radon, through subterranean fissures that develop in the lead-up to the quake. This discharge augments the ionization at the lower atmospheric layers, instigating disturbances that extend from the Earth's surface to the lower ionosphere. A critical component of the LAIC sequence involves the distinctive perturbations of **Extremely Low Electromagnetic Frequencies (ELF)** within the **Schumann Resonances (SR)** spectrum of **2 to 50 Hz**, detectable days ahead of the seismic event. Our study examines 10 earthquakes that transpired over a span of 3.5 months—averaging nearly three quakes monthly—which concurrently generated 45 discernible potential precursor seismic signals. Notably, each earthquake originated in Southern Greece, within a radius of 30 to 250 km from the observatory on Mount Parnon. Our research seeks to resolve two important issues. The first concerns the association between specific ELF signals and individual earthquakes—a question of significant importance in seismogenic regions like Greece, where earthquakes occur frequently. The second inquiry concerns the parameters that determine the detectability of an earthquake by a given station, including the requisite proximity and magnitude. Initial findings suggest that SR signals can be reliably linked to a particular earthquake if the observatory is situated within the earthquake's preparatory zone. Conversely, outside this zone, the correlation becomes indeterminate. Additionally, we observe a differentiation in SR signals based on whether the earthquake took place over land or offshore. The latter category exhibits unique signal behaviors, potentially attributable to the water layers above the epicenter acting as a barrier to the ascending gases, thereby affecting the atmospheric–ionospheric ionization process.

Keywords: Schumann resonances; seismicity; LAIC; electro-seismology

check for updates

Citation: Contopoulos, I.; Mlynarczyk, J.; Kubisz, J.; Tritakis, V. Possible Identification of Precursor ELF Signals on Recent EQs That Occurred Close to the Recording Station. *Atmosphere* **2024**, *15*, 1134. https://doi.org/10.3390/atmos15091134

Academic Editor: Masashi Hayakawa

Received: 26 July 2024
Revised: 9 September 2024
Accepted: 10 September 2024
Published: 19 September 2024

Copyright: © 2024 by the authors. Licensee MDPI, Basel, Switzerland. This article is an open access article distributed under the terms and conditions of the Creative Commons Attribution (CC BY) license (https://creativecommons.org/licenses/by/4.0/).

1. Introduction

The Eastern Mediterranean and especially Greece provides a unique natural setting for studying seismic activity mechanisms. The reason is that South of the island of Crete lies the so-called Mediterranean Ridge which crosses the seafloor from the Ionian islands to the left till the East Mediterranean to the right (Figure 1). Closer to the island of Crete lies the active Hellenic Trench which extends from the Ionian islands to the island of Rhodes. The Mediterranean Ridge is the limit where the Eurasian and African plates collide. These fault lines produce many small and medium magnitude earthquakes (hereafter EQs) of magnitude 3 to 6 on the Richter scale which shake the area very often.

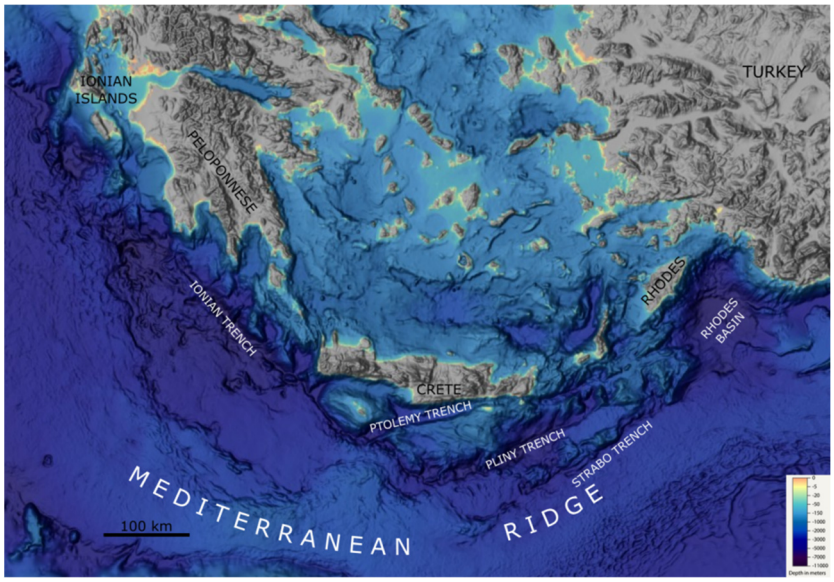

Figure 1. The Mediterranean Ridge and the Hellenic Trench around Crete.

The Greek peninsula is intersected by numerous secondary fault lines, which contribute to the region's robust seismic activity, rendering EQs a frequent occurrence. This regularity provides an abundant source of data for research. Fortunately, the majority of EQs in this area are of low (of magnitude below 3 on the Richter scale) to moderate (3 to 6) intensity. High-magnitude earthquakes (above 6) are rare, and when they do occur, they occur predominantly offshore. Nonetheless, the regularity of seismic events and the resultant damage underscore the critical need for accurate and reliable short-term EQ prediction (lead time of up to one month). According to Sobolev 2015, the two signs of an impending EQ are the progressive movement of fault banks and the associated seismic foreshocks. However, we are still unable to record the movements of deep fault banks and to reliably distinguish foreshocks from unrelated weak earthquakes [1]. In light of the limitations faced by traditional seismological and geological forecasting methods, there is a renewed interest in electro-seismological approaches. This concept, which dates back to the 1960s, gained traction following the observation of ionospheric disturbances preceding a major EQ in Alaska [2,3].

Building on this early work, Hayakawa and Fujinami 1994 [4] laid the groundwork for the discipline now recognized as **electro-seismology**, which was further developed by Hayakawa and Molchanov [5,6]. Pullinets 2018 [7,8] expanded this framework to include the **Lithosphere–Atmosphere–Ionosphere Coupling** (LAIC), integrating electromagnetic phenomena from terrestrial origins to the ionosphere. The central hypothesis of LAIC posits that in the days leading up to an EQ, ionized gases—primarily radon—emanate from subterranean microcracks within the EQ's preparatory zone. This effusion leads to the ionization of the lower atmospheric layers, forming a vertical column reaching up to the lower ionosphere. Empirical support for LAIC was garnered through satellite-detected ionospheric alterations preceding significant seismic events [9–11]. Recent studies, such as Nayak et al., 2023, have expanded on LAIC research by linking seismic b-values and ionospheric changes before the 2023 6.8 Mw Morocco earthquake, demonstrating the connection between the ground and the ionosphere [12]. Similarly, Sharma et al., 2024 analyzed the 2010 7.2 Mw Mexico earthquake and established a strong correlation between TEC and fault lines, thereby validating the LAIC model [13]. Shah et al., 2023 emphasized the synchronization between the atmosphere and ionosphere as earthquake precursors [14], while Shah et al., 2021 extended the research to thermal anomalies observed before earthquakes in Pakistan, further confirming the LAIC mechanism [15]. Additionally,

the remarkable luminous phenomena observed during the earthquakes in Mexico, Morocco, and Fukushima are believed to be manifestations of this process [16].

Following the energization of the preparatory zone surrounding an impending EQ epicenter, a multitude of parameters are impacted, thus being identified as potential quasi-seismic indicators or seismic precursors. The literature is replete with studies on such indicators, including Total Electron Content (TEC), variations in the ionosphere's altitude and density, atmospheric conductivity fluctuations, electromagnetic waves, instabilities, and a range of other disturbances extending from the Earth's surface to the ionosphere and beyond [17–22]. Recent advancements in electro-seismology have incorporated a suite of cutting-edge tools, yielding substantial benefits. Notably, satellite and GPS data, alongside enhancements in software capabilities, sophisticated mathematical models, and machine learning algorithms, were instrumental [23–35].

In the current study, we focus on **ELF electromagnetic waves** as seismic precursors, particularly those within the **Schumann Resonance spectrum range (2–50 Hz)**. Our prior research has demonstrated that surges in ELF activity, specifically in the **20–25 Hz** range, can serve as reliable indicators of an impending earthquake when detected several days in advance [36–43]. This theory was substantiated through extensive testing across 16 medium-magnitude earthquakes that transpired in Southern Greece from **September 2020 to the end of 2021** [42]. Additionally, our empirical analysis suggests that the predictive strength of this precursor is amplified when the EQ epicenter is situated within a **maximum radius of 300 km** from the ELF monitoring station [36–38].

In this article, we address two important questions that have emerged from our own research. Over the now eight years of operation of our SR recording stations, we have observed several instances of abnormal ELF signals in the SR spectrum range. Over all these years, we have been intrigued to find a potential correlation between specific abnormal **SR** ELF signals and individual EQs. It was observed that SR quasi-precursory signals may manifest **1–3 weeks** prior to a significant EQ. However, given the high seismicity of Greece, it is plausible that multiple EQs may occur simultaneously in different locations. This simultaneity complicates the task of attributing a particular SR signal to a specific EQ. Furthermore, assuming that there exists indeed a correlation between abnormal SR signals and EQs, we would like to know how close to our recording site must the EQ take place for the precursor SR signal to be distinctly captured.

2. Outline of the ELF(SR) and Their Relation to Geophysics

The ELF band is the low range of the electromagnetic spectrum which extends from 0.3 to 300 Hz. The very low part of this band, from 2 to 50 Hz, is the so-called Schumann part where Schumann's resonances (SR) are observed. It is formed by radio waves that propagate around the Earth several times before fading away. Schumann resonances (SRs) are quasi-standing electromagnetic waves that form in the spherical cavity between the surface of the Earth and the lower layers of the ionosphere. This spherical area is a natural waveguide that acts as a resonance cavity for ELF electromagnetic waves. The source of these waves is global lightning discharges, which act like antennas emitting electromagnetic waves into the Earth–ionosphere cavity. The German scientist Otto Schumann calculated the resonant frequencies for the Earth-ionosphere cavity as follows: he predicted theoretically that for a perfect spherical electromagnetic resonance cavity of radius α, the relevant frequencies f_n are given by the expression [39].

$$f_n = \frac{c}{2\pi\alpha}\sqrt{n(n+1)} \quad (1)$$

where c is the speed of light, and α is the Earth's radius. $n = 1$ corresponds to the fundamental mode frequency, $n = 2$ to the second mode frequency, etc. The theoretical frequencies obtained from Equation (1) are equal to 10.6, 18.3, 25.9, 33.5, and 41.0 Hz. Indeed, the first experimental measurements of the Schumann resonances, performed in New England on the 27–28 of June 1960 by Balser and Wagner [40,41], showed that the Schumann resonance

frequencies were equal to 7.8, 14.2, 19.6, 25.9, and 32 Hz. The difference from the theoretical calculation of Schumann is linked to the imperfect nature of the Earth-ionosphere cavity. This is because the Earth–ionosphere cavity is not a perfect resonance cavity, and the propagation velocity of the ELF waves in the atmosphere is slower than the speed of light in vacuum. In particular, the upper boundary of the Earth–ionosphere cavity differs a lot from a perfect conductor (the atmospheric conductivity increases with the altitude and reaches significant values for the ELF waves in the lower ionosphere). The propagation velocity of ELF waves decreases with frequency and is different on the dayside of Earth than on the night side. Moreover, the ELF wave propagation constant (or transmission parameter) depends on the atmospheric vertical conductivity profiles $\sigma(h)$ for the daytime and night-time conditions. The main source of Schumann resonances is lightning activity, which is mainly due to the high frequency of thunderstorms occurring in the tropical belt around the world, creating electromagnetic waves that propagate within the cavity [40,41].

Over the last thirty years, the interest in SR has increased due to strong evidence that they correlate with several geophysical and biological phenomena, including EQs, which are the focus of many articles and reviews. There is a great expansion of the SR applications related to many geophysical and biological phenomena like thunderstorms, global lightning, global temperature, El Nino/Nina, human brain rhythms, solar proton events, and certainly the main subject of the present paper which is the detection of precursory signals of a forthcoming seismic activity. Closing this paragraph, we cite a number of articles that present various types of seismic precursors [42–47].

3. Questions and Possible Answers

We have already mentioned that Greece, located in the East Mediterranean, experiences a high number of low-to-medium-magnitude EQs. This is due to the very active seismic arc known as the Hellenic Trench, located southeast of the island of Crete, where the European and African tectonic plates collide (Figure 1). Approximately 60% of global seismic activity occurs in this area, with most of it happening offshore, which protects the wider area from catastrophes. EQs with magnitudes between 3 and 6.5 on the Richter scale, originating from the Hellenic arc or other secondary faults in the Greek area, occur frequently, making it an important point of research for earthquake prediction. The idea of a relationship between EQs and atmospheric electricity was very attractive some years ago. This is why we started planning the systematic recording, archiving, and study of ELF/SR (2–50 Hz) measurements.

As we stated in the Introduction, SR measurements play a very important role in EQ prediction in the framework of Lithosphere–Atmosphere–Ionosphere Coupling (LAIC). The most difficult part of obtaining SR measurements is to find a proper place for the installation of the recording site. SR recordings are extremely sensitive to any kind of anthropogenic activity and electromagnetic interferences caused by power lines, mobile phone antennas, etc. We described in detail these difficulties in two extended publications [48,49]. After a long series of tests in various places, we were able to find two proper sites, one in Northern Greece close to the town of Kalpaki near the Albanian border, and a second site in the south on Mount Parnon near the town of Sparta. In the present work, we use information coming from the south site because the seismic activity we study is concentrated in the south. Thanks to the contribution of the forest service of the town of Sparta, we were able to build an installation on Mount Parnon (1450 m) which lies in a very isolated and uninhabited location. The area fulfills all the criteria for the recording of good quality SR data (isolation, electromagnetic clearance, etc.), while a very strong building guarantees safety from undesired visits. Inside the building, there is a complete recording system of the AGH University of Krakow with two coils oriented in the North–South and East–West directions as well as two Greek systems, one with a single coil in the North–South direction and one with two coils also oriented in the North–South and East–West directions. Due to technical problems, in the present study, we are going to use data coming from the

Polish system of the AGH University of Krakow. The interested reader may find extensive descriptions of the area and the installed recording systems in [50–54].

As a short introduction, we present below figures that make clear what is a normal SR recording and what we consider a potential precursor seismic signal. In Figures 2 and 3, typical recordings by both recording systems received at the same time are depicted. Figure 2 represents typical SR recordings while Figure 3 represents abnormal signals recorded by both systems that may constitute potential seismic precursors.

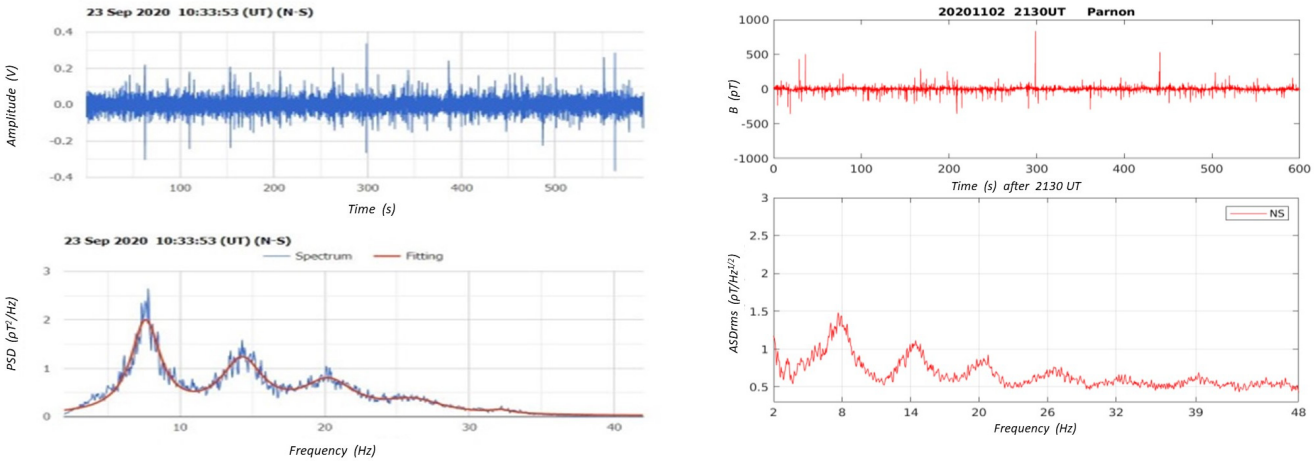

Figure 2. Typical ELF recordings 0–50 Hz, raw data (upper panels) and associated Fourier spectra (low panels), received by both the Greek (**left**) and the Polish (**right**) systems in our observing site on Mount Parnon. Schumann's resonances around 7, 14, 21, and 28 Hz are evident in both spectra. PSD stands for "Power Spectral Density" in the Greek system recording (**left**). ASD stands for "Amplitude Spectral Density" in the Polish system recording (**right**). B stands for the magnetic field value (in pT). N–S denotes recordings from the North–South oriented coil.

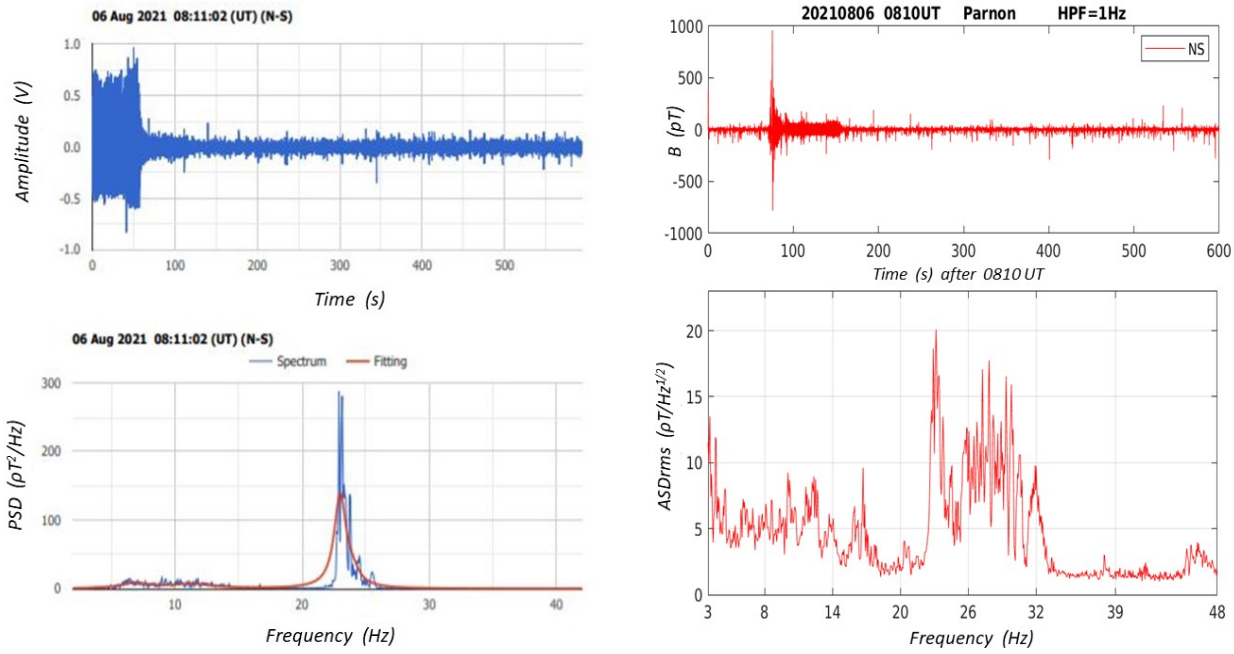

Figure 3. Typical strong perturbations in the raw data and spectra are considered potential precursor seismic signals. Simultaneous measurements were received by the Greek (blue) and the Polish (red) systems, respectively.

There are three questions at this stage. If the LAIC scenario is realistic, we would like to know the following:

1. How far from the recording station could the epicenter of an EQ be located for this to produce an observable precursor signal?
2. How strong it must be for precursor signals to be recorded?
3. How can we associate a recorded signal with a certain EQ?

Since the application of the LAIC scenario starts with the emergence of ionizing gases from fissures/microcracks in the ground several days before the occurrence of an EQ, **the preparation zone of an EQ is identified as a key parameter of the whole process**. We have already mentioned that 2 to 3 weeks before an EQ a preparation zone is generated around its epicenter, the extent of which is relevant to the magnitude of the future EQ. The radius of this area may be estimated by the empirical formula

$$R_{preparation\ zone} = 10^{0.43M}(\text{km}), \quad (2)$$

introduced by Dobrowolsky et al. 2007, where M is the magnitude of the earthquake on the Richter scale [55]. In other words, it is implied that, according to the LAIC scenario, an EQ can give precursory signals which may be recorded by the SR station only if

$$Distance \leq R_{preparation\ zone} \quad (3)$$

The problem is that precursor signals coming from a preparation zone appear up to twenty days in advance before an EQ occurrence, and two or three more EQs may occur in various places around the recording station within this time span. Therefore, the main question that we need to answer is how we can identify the certain EQ that produced a certain precursor SR signal. A set of recent low to medium EQs tabulated in Table 1 which occurred during the first four months of 2024 in the south of the Greek peninsula could help shed some light on the above questions.

Table 1. EQs which occurred around the Mount Parnon recording station during a strong sequence of seismic activity in the first semester of 2024. The preparation zone is obtained by Equation (2), and the actual distance is expressed in km along an approximately straight line between the EQ epicenter and our recording station.

A/A	Date	Place	Magnitude (Richter)	Preparation Zone (km)	Distance (km)
1	16 January 2024	Leonidion	4.8	111.17	30
2	18 January 2024	Kymi	4.8	111.17	170
3	22 January 2024	Kammena Vourla	4.1	57.94	165
4	22 February 2024	Itea	4.4	77.98	108
5	22 February 2024	Kyparissia Gulf	4.4	77.98	106
6	2 March 2024	Farsala	4.1	57.94	226
7	3 March 2024	Kefalonia	3.5	26.24	226
8	29 March 2024	Kyparissia Gulf	5.6	255.85	106
9	29 April 2024	Hrakleio	4.2	63.97	312
10	13 May 2024	Zacharo	3.7	38.99	98

In Table 1, 10 EQs of magnitude from 3.3 to 5.8 on the Richter scale were listed. The specific characteristics of these EQs are that (a) they occurred from the 16th of January 2024 to the 13th of May of the same year (this corresponds to about 2.5 EQs per month on average), and (b) they occurred very close to the recording station on Mount Parnon. The closest EQ took place a few kilometers away (no. 1 in Table 1), while the most distant took place 312 km away (no. 9 in Table 1).

The epicenters of the EQs listed in Table 1 (yellow pins), as well as the position of the recording site (lower red pin) are also shown in Figure 4. The color circles around the recording station on Mount Parnon (red pin) indicate the radius of the preparation zones if the position of the station were the EQ epicenter. The outer red circle corresponds to an EQ of magnitude 6 on the Richter scale, while the inner blue circle corresponds to an EQ of magnitude 4. The other circles differ by 0.5 Richter from one another. From this figure, it is clear that an EQ that may occur in Heraklion on the island of Crete should have a magnitude of at least 6 on the Richter scale in order to be recorded by the station on Mount Parnon. The same applies to Kalpaki of Ioannina in the North of Greece (upper red pin in Figure 4).

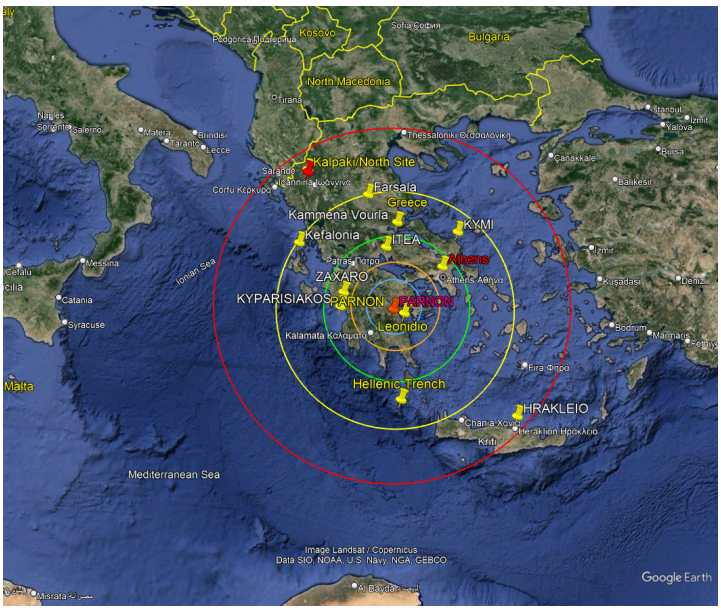

Figure 4. Greek peninsula with the recording station of Parnon (red pin in the center of the circles) and the 10 EQs of Table 1 (yellow pins) shown. The color circles delimit the preparation areas around the station if the EQ epicenter lies at the position of the station itself. The outer red circle corresponds to an EQ of 6 Richter while the inner blue circle corresponds to an EQ of 4 Richter. Overall, the shown circles delimit zones of EQs = 6, 5.5, 5.0, 4.5 and 4 Richter from the outer to the inner circle, respectively.

Precursor signals related to the set of EQs presented in Table 1 started to be recorded close to the end of December 2023 (23 December 2023). Since then, we recorded one to two signals every day till EQ no.1 of Table 1 (Leonidion) occurred. This was a very characteristic EQ because the epicenter was located just 30 km from the recording site of Parnon. In Figure 5, we present the first signal on the 23 December 2023, and the last signal on the 11 January 2024, five days before the main EQ occurrence. Between these two signals, one to two signals of this type were recorded every day.

It is clear that if we apply the empirical relation introduced by Dobrowolsky et al., 2007 (Equation (2)), only two of the EQs listed in Table 1 would have produced precursor signals detectable from our observing station on Mount Parnon. These are EQ no. 1 at Leonidion (the distance of 30 km was much shorter than the preparation zone corresponding to its magnitude, namely 111 km), and no. 8 at the Kyparissia Gulf (this EQ was strong enough to generate a large preparation zone of 256 km which encompassed our observing station at 106 km). According to Equation (2), all the other EQ-generated precursor signals would not be detectable from our observing station.

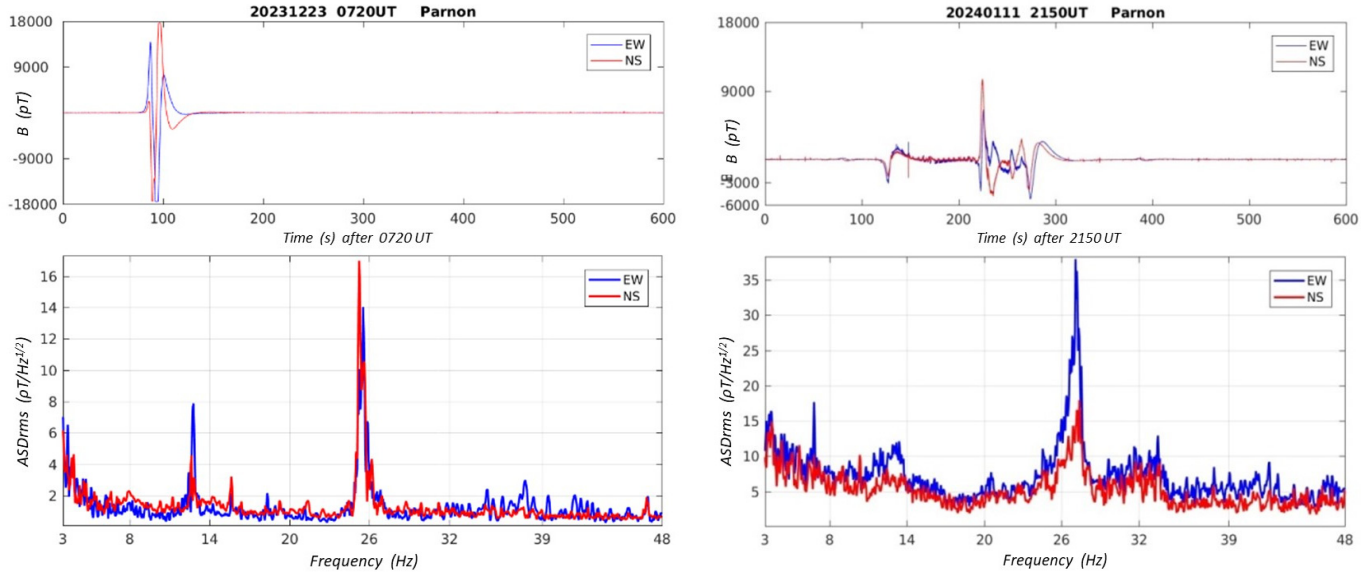

Figure 5. The first (**left**) and the last (**right**) recorded potential precursor signals before the EQ at Leonidion (no.1 in Table 1). E–W denotes recordings from the East–West oriented coil.

In Figure 6, we present the last three particular signals recorded six days before the 5.8 Richter EQ, which occurred in the Kyparissia Gulf (or Kyparissiakos). The specificity of these signals is the double excess which probably has to do with the fact that it took place offshore.

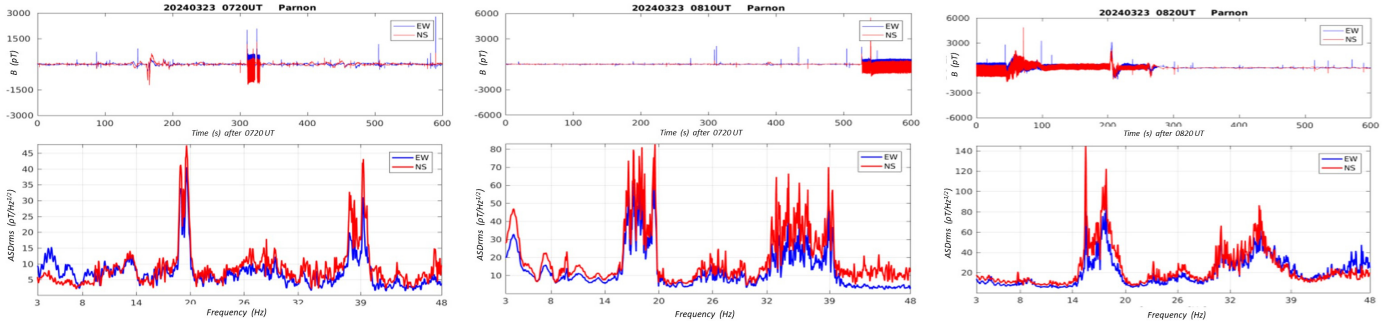

Figure 6. The last 3 successive signals before the 5.6 R EQ in the Kyparissia Gulf (no. 7 in Table 1). The spectrum of these signals differs from the spectrum of the signals in Figure 5 (they show two characteristic excesses at the boundaries of the normal precursor frequency area of 20–25 Hz).

It is clear that the signals in Figure 6 are different from the signals in Figure 5. In fact, most recorded precursor signals associated with the Kyparissia Gulf EQ have similar features. Their spectrum shows two characteristic strong excesses at the boundaries of the frequency area of 20–25 Hz where precursor signals from standard land EQs normally lie. We offer a tentative explanation for this difference, namely that it is due to the offshore origin of the Kyparissia Gulf EQ. This interesting observation leads us to suggest that EQ signals with an offshore origin need additional investigation.

4. Discussion

Assuming the validity of the LAIC scenario and the empirical relation of Equation (3), we could come up with some interesting results from Table 1. At first, it is clear that precursor signals may be recorded only if the recording stations are inside the corresponding EQ preparation zone. Under this condition, only 2 out of the 10 EQs of Table 1 satisfy this criterion. These are EQ no. 1, which occurred in the town of Leonidion very close to the recording site (about 30 km in a straight line), and EQ no. 8 which occurred on the seafloor

of Kyparissia Gulf. All the other eight EQs do not satisfy the requirement of Equation (3). One thus expects that their precursor signals are not recordable from the Mount Parnon station. Nevertheless, 45 signals were recorded between the first signal of EQ no. 1 and the last signal in April 2024. These signals need identification.

In Table 2, these 45 signals are divided into seven time intervals. The first time interval contains 26 signals which were recorded in the preparation time before the main EQ no. 1 at Leonidion. The second time interval contains seven signals that occurred in the next two weeks after the main EQ at Leonidion and they seem to be produced by the meta-seismic sequence of weaker EQs that always follow a main EQ. Clear signals during the meta-seismic sequence of a medium magnitude EQ, which occurred very near the recording site, were also detected in August of 2019 when a 5.8 magnitude EQ took place near the North recording site in Kalpaki (upper red pin in Figure 2) [36].

Table 2. Frequency of potential EQ precursor signals in the interval 23/12/23 to 13/5/24.

A/A	**1**	**2**	**3**	**4**	**5**	**6**	**7**
DATES	23/12/24–16/1/24	17/1/24–29/1/24	30/1/24–10/3/24	11/3/24–24/3/24	25/3/24–30/3/24	31/3/24–14/4/24	15/4/24–13/5/24
No. of signals	**26**	**7**	**0**	**7**	**0**	**5**	**0**
	Associated with EQ no. 1 in Leonidion			**Associated with EQ no. 8 in the Kyparissia Gulf**			

After that, no abnormal signals were observed for more than a month (time interval 3), although, according to Table 1, several EQs occurred in that time period. Those, however, were outside their corresponding preparation zones and Equation (3) was not satisfied (i.e., the corresponding preparation distances in Table 1 were smaller than the corresponding distances from our observing station); therefore, we did not expect to observe any precursor signals from them.

The fourth time interval contains seven potential precursor signals that appeared before the main EQ in the Kyparissia Gulf (no. 6 in Table 1), and the five signals in the sixth time interval probably belong to the meta-seismic sequence of the main EQ no. 6. It is very interesting that no abnormal signals were recorded in the days immediately before and after EQ no. 6 (fifth time interval). Finally, while two more EQs occurred in the seventh time interval, no abnormal signals were recorded, probably because these EQs took place too far from our SR recording station. In the context of the LAIC scenario, the above may be attributed to the disturbance of the Earth–ionosphere cavity (e.g., due to radon emission) over a finite region around the EQ (the extent of which is determined by Equation (2)) a few days before and after the EQ.

5. Conclusions

The main results of this study may be summarized as follows:

a. Abnormal SR signals detected 1 to 3 weeks before a main EQ may be considered seismic precursors only when the recording site is located inside the preparation zone of the EQ.
b. The closer the EQ is to the recording site, the more unambiguous the precursor signals are.
c. Signals produced by offshore EQs seem to contain Fourier frequencies divided into two parts at the two ends of the normal range of 20 to 25 Hz. This peculiar feature may be related to the water layers above an offshore EQ which constitute an obstacle to the emanating gases, causing this way retardation in the atmospheric–ionospheric ionization. Additional study of abnormal SR signals produced by offshore EQs is necessary.

In summary, **Schumann Resonance (SR) pre-seismic signals** prior to a major earthquake (EQ) offer valuable insights, especially when the EQ's preparation zone encompasses

the recording site. Unfortunately, due to the limitations of current SR signal interpretations, they cannot yet be considered definitive indicators of an imminent seismic event. These signals are significant pieces of the puzzle within the **Lithosphere–Atmosphere–Ionosphere Coupling (LAIC)** framework. A reliable and accurate seismic forecast will only be feasible when the entirety of data pertinent to the LAIC model is meticulously collected, scrutinized, and analyzed using sophisticated software. We believe there is significant potential in future research and technological advances for a more reliable earthquake prediction.

Author Contributions: Conceptualization, V.T.; methodology, I.C. and V.T.; formal analysis, I.C. and V.T.; investigation, J.M. and V.T.; resources, J.M., J.K. and V.T.; writing—original draft preparation, V.T.; writing—review and editing, I.C. and V.T.; supervision, I.C. All authors have read and agreed to the published version of the manuscript.

Funding: This research was partially funded by the Research Commission of the Academy of Athens and the Mariolopoulos-Kanaginis Foundation for Environmental Science.

Institutional Review Board Statement: Not applicable.

Informed Consent Statement: Not applicable.

Data Availability Statement: The data presented in this study are available on request from the corresponding author.

Acknowledgments: We are deeply indebted to the forest service of Lakonia prefecture in the town of Sparta, especially G. Zakkas and the forest personnel, S. Petrakos, K. Samartzis, N. Sourlis, and K. Tsagaroulis for their valuable contribution in the establishment and servicing of our South Observation Site near the village of Vamvakou, on Mount Parnon. We would also like to address a warm thank you to the Mariolopoulos–Kanaginis Foundation for Environmental Sciences for its financial support, as well as to the Research Committee of the Academy of Athens for supplementary support.

Conflicts of Interest: The authors declare no conflicts of interest.

References

1. Sobolev, G.A. Methodology, Results, and Problems of Forecasting Earthquakes. *Her. Russ. Acad. Sci.* **2015**, *85*, 107. [CrossRef]
2. Davis, K.; Baker, D.M. Ionospheric effects observed around the time of the Alaska earthquake of March 28, 1964. *J. Geophys. Res.* **1965**, *70*, 2251–2253. [CrossRef]
3. Leonard, R.S.; Barnes, R.A., Jr. Observation of ionospheric disturbances following the Alaska earthquake. *JGR Lett.* **1965**, *70*, 1250–1253. [CrossRef]
4. Hayakawa, M.; Fujinawa, Y. (Eds.) *Electromagnetic Phenomena Related to Earthquake Prediction*; Terra Scientific Publishing Company: Tokyo, Japan, 1994.
5. Hayakawa, M.; Molchanov, O. (Eds.) *Seismo-Electromagnetics: Lithosphere-Atmosphere-Ionosphere Coupling*; Terra Scientific Publiching Company: Tokyo, Japan, 2002.
6. Hayakawa, M.; Molchanov, O.A. Seismo-electromagnetics: As a new field of radiophysics: Electromagnetic phenomena associated with earthquakes. *URSI Radio Sci. Bull.* **2007**, *2007*, 8–17.
7. Pullinets, A.S. Lithosphere-Atmosphere-Ionosphere Coupling Related to Earthquakes. In Proceedings of the 2nd URSI AT-OASC, Gran Canaria, Spain, 28 May–June 2018.
8. Pulinets, S.; Ouzounov, D. Intergeospheres Interaction as a source of earthquake precursor's generation. In Proceedings of the EMSEV 2018 International Workshop, Potenza, Italy, 17–21 September 2018.
9. Zhao, B.; Qian, C.; Yu, H.; Liu, J.; Maimaitusun, N.; Yu, C.; Zhang, X.; Ma, Y. Preliminary analysis of ionospheric anomalies before strong earthquakes in and around mainland China. *Atmosphere* **2022**, *13*, 410. [CrossRef]
10. Hayakawa, M.; Tomakazu, A.; Rozhnoi, A.; Solovieva, M. Very -low -to Low-Frequency Sounding of Ionospheric Perturbations and Possible Association with Earthquakes in Pre-Earthquake Processes: A Multidisciplinary Approach to Earthquake Prediction Studies. *Geophys. Monogr.* **2018**, *234*, 277–304.
11. Namgaladge, A.; Karpov, M.; Knyazeva, M. Seismogenic disturbances of the ionosphere during high geomagnetic activity. *Atmosphere* **2019**, *10*, 359. [CrossRef]
12. Nayak, K.; Lopez-Urias, C.; Romero-Andrade, R.; Sharma, G.; Guzman-Acevedo, G.M.; Trejo-Soto, M.E. Ionospheric Total Electron Content (TEC) Anomalies as Earthquake Precursors: Unveiling the Geophysical Connection Leading to the 2023 Moroccan 6.8 Mw Earthquake. *Geosciences* **2023**, *13*, 319. [CrossRef]
13. Sharma, G.; Nayak, K.; Romero-Andrade, R.; Aslam, M.A.; Sarma, K.K.; Aggarwal, S.P. Low Ionosphere Density Above the Earthquake Region of Mw 7.2, El Mayor-Cucapah Earthquake Evident from Dense CORS Data. *J. Indian Soc. Remote Sens.* **2024**, *52*, 543. [CrossRef]

14. Shah, M.; Shahzad, R.; Jamjareegulgarn, P.; Ghaffar, B.; Oliveira-Junior, J.F.; Hassan, A.M.; Ghamry, N.A. Machine-Learning-Based Lithosphere-Atmosphere-Ionosphere Coupling Associated with Mw > 6 Earthquakes in America. *Atmosphere* **2023**, *14*, 1236. [CrossRef]
15. Shah, M.; Qureshi, R.-U.; Khan, N.G.; Ehsan, M.; Yan, J. Artificial Neural Network based thermal anomalies associated with earthquakes in Pakistan from MODIS LST. *J. Atmos. Sol.-Terr. Phys.* **2021**, *215*, 105568. [CrossRef]
16. Xie, B.; Wu, L.; Mao, W.; Wang, Z.; Sun, L.; Xu, Y. Horizontal Magnetic Anomaly Accompanying the Co-Seismic Earthquake Light of the M7.3 Fukushima Earthquake of 16 March 2022 Phenomenon and Mechanism. *Remote Sens.* **2023**, *15*, 5052. [CrossRef]
17. Sorokin, M.V.; Pokhotelov, A.O. Gyrotropic Waves in the mid-latitude ionosphere. *J. Atmos. Sol.-Terr. Phys.* **2005**, *67*, 921–930. [CrossRef]
18. Hayakawa, M.; Ohta, K.; Sorokin, M.V.; Yaschenko, K.A.; Izutsu, J.; Hobara, Y.; Nickolaenko, P.A. Interpretation in terms of gyrotropic waves of Schumann –resonance-like line emissions observed at Nakatsugawa in possible association with nearby Japanese earthquakes. *J. Atmos. Terr. Phys.* **2010**, *72*, 1292–1298. [CrossRef]
19. Chakrabarti, S.; Saha, M.; Khan, R.; Mandal, S.; Acharyya, K.; Saha, R. Possible detection of ionospheric disturbances during Sumatra Andaman islands earthquakes in December. *Indian J. Radio Space Phys.* **2005**, *34*, 314–317.
20. Sorokin, V.M.; Hayakawa, M. On the generation of narrow -banded ULF/ELF pulsations in the lower ionospheric contacting layer. *J. Geophys. Res.* **2008**, *113*, A06306. [CrossRef]
21. Chakrabarti, S.K.; Sasmal, S.; Chakrabarti, S. Ionospheric anomaly due to seismic activities part 2: Evidence from d-layer preparation and disappearance times. *Nat. Hazards Earth Syst. Sci.* **2010**, *10*, 1751–1757. [CrossRef]
22. Harrison, G.R.; Aplin, L.K.; Rycroft, J.M. Atmospheric electricity coupling between earthquake regions and the ionosphere. *J. Atmos. Sol.-Terr. Phys.* **2010**, *72*, 376–381. [CrossRef]
23. Shah, M.; Jin, S. Pre-seismic ionospheric anomalies of the 2013 Mw 7.7 Pakistan earthquake from GPS and COSMIC observations. *Geod. Geodyn.* **2018**, *9*, 378–387. [CrossRef]
24. Liu, J.Y.; Chuo, Y.J.; Shan, S.J.; Tsai, Y.B.; Chen, Y.I.; Pulinets, S.A.; Yu, S.B. Pre-earthquake ionospheric anomalies registered by continuous GPS TEC measurements. *Ann. Geophys.* **2004**, *22*, 1585–1593. [CrossRef]
25. Tsugawa, T.; Saito, A.; Otsuka, Y.; Nishioka, M.; Maruyama, T.; Kato, H.; Nagatsuma, T.; Murata, K.T. Ionospheric disturbances detected by GPS total electron content observation after the 2011 off the Pacific coast of Tohoku Earthquake. *Earth Planets Space* **2011**, *63*, 875–879. [CrossRef]
26. Dong, L.; Zhang, X.; Du, X. Analysis of Ionospheric precursors possibly related to Yangbi Ms 6.4 and Maduo Ms 7.4 earthquake occurred on 21st May, 2021 in China by GPS TEC and GIM TEC data. *Atmosphere* **2022**, *13*, 1725. [CrossRef]
27. Walker, S.N.; Kadirkamanathan, V.; Pokhotelov, O.A. Changes in the ultra-low frequency wave field during the precursor phase to the Sichuan earthquake: DEMETER observations. *Ann. Geophys.* **2013**, *31*, 1597–1603. [CrossRef]
28. Parrot, M.; Li, M. DEMETER Results Related to Seismic Activity. *URSI Radio Sci. Bull.* **2017**, *88*, 18–25.
29. Li, M.; Shen, X.; Yu, C.; Zhang, X.; Zhang, Y.; Yu, C.; Yan, R.; Liu, D.; Lu, H.; Guo, F.; et al. Primary joint statistical seismic influence on ionospheric parameters recorded by the CSES and DEMETER satellites. *J. Geophys. Res. Space Phys.* **2020**, *125*, e2020JA028116. [CrossRef]
30. De Santis, A.; Balasis, G.; Pav'on-Carrasco, F.J.; Cianchini, G.; Mandea, M. Potential earthquake precursory pattern from space: The 2015 Nepal event as seen by magnetic Swarm satellites. *Adv. Space Res.* **2017**, *461*, 119–126. [CrossRef]
31. Li, M.; Yang, Z.; Song, J.; Zhang, Y.; Jiang, X.; Shen, X. Statistical Seismo-Ionospheric influence with focal Mechanism under consideration. *Atmosphere* **2023**, *14*, 455. [CrossRef]
32. Florios, K.; Contopoulos, I.; Christofilakis, V.; Tatsis, G.; Chronopoulos, S.; Repapis, C.; Tritakis, V. Pre-seismic Electromagnetic Perturbations in Two Earthquakes in Northern Greece. *Pure App. Geophys.* **2020**, *177*, 787–799. [CrossRef]
33. Florios, K.; Contopoulos, I.; Tatsis, G.; Christofilakis, V.; Chronopoulos, S.; Repapis, C.; Tritakis, V. Possible Earthquake Forecasting in a narrow Space-Time-Magnitude Window. *Earth Sci. Inform.* **2021**, *14*, 349–364. [CrossRef]
34. Karamanos, K.; Peratzakis, A.; Kapiris, P.; Nikolopoulos, S.; Kopanas, X.; Eftaxias, K. Extractihg preseismic electromagnetic, signatures in terms of symbolic dynamics. *Nonlinear Process. Geophys.* **2005**, *12*, 835–848. [CrossRef]
35. Karamanos, K.; Dakopoulos, D.; Aloupis, K.; Peratzakis, A.; Athanasopoulou, L.; Nikolopoulos, S.; Kapiris, P.; Eftaxias, K. Study of pre-seismic Electromagnetic signals in terms of complexity. *Phys. Rev. E* **2006**, *74*, 016104. [CrossRef] [PubMed]
36. Christofilakis, V.; Tatsis, G.; Votis, G.; Contopoulos, I.; Repapis, C.; Tritakis, V. Significant ELF perturbations in the Schumann Resonance band before and during a shallow mid-magnitude seismic activity in the Greek area (Kalpaki). *J. Atmos. Sol.-Terr. Phys.* **2019**, *182*, 138–146. [CrossRef]
37. Tritakis, V.; Contopoulos, I.; Mlynarczyk, J.; Christofilakis, V.; Tatsis, G.; Repapis, C. How Effective and Prerequisite Are Electromagnetic Extremely Low Frequency (ELF) Recordings in the Schumann Resonances Band to Function as Seismic Activity Precursors. *Atmosphere* **2022**, *13*, 185. [CrossRef]
38. Tritakis, V.; Mlynarczyk, J.; Contopoulos, I.; Kubisz, J.; Christofilakis, V.; Tatsis, G.; Chronopoulos, S.K.; Repapis, C. Extremely low frequency (ELF) electromagnetic signals as a possible precursory warning of incoming seismic activity. *Atmosphere* **2024**, *15*, 457. [CrossRef]
39. Schumann, W.O. On the free oscillations of a conducting sphere which is surrounded by an air layer and an ionosphere shell. *Z. Naturforschaftung* **1952**, *7*, 149–154. (In German) [CrossRef]
40. Balser, M.; Wagner, C. Observations of Earth–Ionosphere Cavity Resonances. *Nature* **1960**, *188*, 638–641. [CrossRef]

41. Balser, M.; Wagner, C.A. Diurnal power variations of the Earth-ionosphere cavity modes and their relationship to worldwide thunderstorm activity. *J. Geophys. Res.* **1962**, *67*, 619–625. [CrossRef]
42. Nickolaenko, P.A.; Galuk, P.Y.; Hayakawa, M. The effect of a compact ionosphere disturbance over the earthquake: A focus on Schumann resonance. *Int. J. Electron. Appl. Res.* **2018**, *5*, 11–39. [CrossRef]
43. Schekotov, A.; Chebrov, D.; Hayakawa, M.; Belyaev, G.; Berseneva, N. Short-term earthquake prediction in Kamchatka using low-frequency magnetic fields. *Nat. Hazards* **2020**, *100*, 735–755. [CrossRef]
44. Sekiguchi, M.; Hobara, Y.; Hayakawa, M. Diurnal and seasonal variations in the Schumann resonance parameters at Moshiri, Japan. *J. Atmos. Electr.* **2008**, *28*, 1–10. [CrossRef]
45. Roldugin, V.; Maltsev, Y.P.; Petrova, G.; Vasiljev, A. Decrease of the first Schumann resonance frequency during solar proton events. *J. Geophys. Res. Space Phys.* **2001**, *106*, 18555–18562. [CrossRef]
46. Sinitsind, V.; Gordeev, E.; Hayakawa, M. Seismoionospheric depression of the ULF geomagnetic fluctuations at Kamchatka and Japan. *Phys. Chem. Earth* **2006**, *31*, 313–318.
47. Fidani, C.; Battiston, R. Analysis of NOAA particle data and correlations to seismic activity. *Nat. Hazards Earth Syst. Sci.* **2008**, *8*, 1277–1291. [CrossRef]
48. Tritakis, V.; Contopoulos, I.; Florios, C.; Tatsis, G.; Christophylakis, V.; Baldoumas, C.; Repapis, C. Anthropogenic Noise and its Footprint on ELF Schumann Resonance Recordings. *Front. Earth Sci.* **2021**, *9*, 646277. [CrossRef]
49. Mlynarczyk, J.; Tritakis, V.; Contopoulos, I.; Nieckarz, Z.; Christophilakis, V.; Tatsis, G.; Repapis, C. Anthropogenic Sources of Electromagnetic Interferences in the Lowest Elf Band Recordings (Schumann Resonances). *Magnetism* **2022**, *2*, 152–167. [CrossRef]
50. Tatsis, G.; Votis, C.; Christofilakis, V.; Kostarakis, P.; Tritakis, V.; Repapis, C. A prototype data acquisition and processing system for Schumann resonance measurements. *J. Atmos. Sol.-Terr. Phys.* **2015**, *135*, 152–160. [CrossRef]
51. Tatsis, G.; Christofilakis, V.; Chronopoulos, S.K.; Kostarakis, P.; Nistazakis, H.E.; Repapis, C.; Tritakis, V. Design and Implementation of a Test Fixture for ELF Schumann Resonance Magnetic Antenna Receiver and Magnetic Permeability Measurements. *Electronics* **2020**, *9*, 171. [CrossRef]
52. Tatsis, G.; Christofilakis, V.; Chronopoulos, S.K.; Baldoumas, G.; Sakkas, A.; Paschalidou, A.K.; Kassomenos, P.; Petrou, I.; Kostarakis, P.; Repapis, C.; et al. Study of the variations in THE Schumann resonances parameters measured in a Southern Mediterranean environment. *Sci. Total Environ.* **2020**, *715*, 136926. [CrossRef]
53. Votis, C.I.; Tatsis, G.; Christofilakis, V.; Chronopoulos, S.K.; Kostarakis, P.; Tritakis, V.; Repapis, C. A new portable ELF Schumann resonance receiver: Design and detailed analysis of the antenna and the analog front-end. *J. Wirel. Commun. Netw.* **2018**, *2018*, 155. [CrossRef]
54. Mlynarczyk, J.; Popek, M.; Kulak, A.; Klucjasz, S.; Martynski, K.; Kubisz, J. New Broadband ELF Receiver for Studying Atmospheric Discharges in Central Europe. In Proceedings of the Baltic URSI Symposium, Poznan, Poland, 14–17 May 2018.
55. Dobrovolsky, I.P.; Zubkov, S.I.; Miachkin, V.I. Estimation of the size of earthquake preparation zones. *Pure Appl. Geophys.* **1979**, *117*, 1025–1044. [CrossRef]

Disclaimer/Publisher's Note: The statements, opinions and data contained in all publications are solely those of the individual author(s) and contributor(s) and not of MDPI and/or the editor(s). MDPI and/or the editor(s) disclaim responsibility for any injury to people or property resulting from any ideas, methods, instructions or products referred to in the content.